Desalination and Water Treatment
www.deswater.com
doi: 10.5004/dwt.2022.28564

262 (2022) 137–151
June

Investigation of the cellulose reed plant as a potential adsorbent to remove Pb(II): equilibrium isotherms and thermodynamic studies

Abdelhay El Amri[a], Jaouad Bensalah[a,*], Lamya Kadiri[a], Youness Essaadaoui[a], Imane Lebkiri[a], Abdelkader Zarrouk[b], El Housseine Rifi[a], Ahmed Lebkiri[a]

[a]*Laboratory of Advanced Materials and Proceeding Engineering (LAMPE), Department of Chemistry, Faculty of Sciences, Ibn Tofail University, B.P. 133, 14000 Kenitra, Morocco, emails: bensalahjaouad11@gmail.com (J. Bensalah), elamriabdelhay@gmail.com (A. El Amri), kadiri.lamya@gmail.com (L. Kadiri), essaadaouiy@gmail.com (Y. Essaadaoui), imanelebkiri@gmail.com (I. Lebkiri), elhosseinr@yahoo.fr (E. Housseine Rifi), lebkiriahm@yahoo.fr (A. Lebkiri)*
[b]*Laboratory of Materials, Nanotechnology and Environment, Faculty of Sciences, Mohammed V University in Rabat, Av. Ibn Battouta, P.O. Box: 1014, Agdal-Rabat, Morocco, email: azarrouk@gmail.com*

Received 17 December 2021; Accepted 19 April 2022

ABSTRACT

In this work, we presented a study on the solid phase adsorption of Pb(II) ion by raw cellulose (CB) and by modified cellulose (CM). The metal Pb(II) adsorption mechanism was also interpreted by Fourier-transform infrared spectroscopy and energy-dispersive X-ray spectroscopy. The most important results for this adsorption can be summarized to: The effect of some experimental parameters was studied using the adsorption technique. Have shown that the retention of Pb(II) pollutant is a little fast where the equilibrium is reached after 90 min for CB and 70 min for CM. The kinetics of adsorption on the cellulose ligand, show that this support is a good adsorbent of Pb(II) in aqueous solution. This kinetics are influenced by the studied parameters, temperature and pH, the mass of the support and the initial concentration. The pH of the aqueous phase is between 4.5 and 6. The increase of the pH of the aqueous phase after adsorption shows that the extraction is done, in addition to the adsorption, by competition between the resin and the aqueous phase rich in Pb^{2+}. Increasing the temperature of the aqueous phase-resin mixture from 25°C to 65°C increases the adsorption yield and sorption capacity. This proper that the adsorption is endothermic. The adsorption capacity increases with increasing initial lead concentration and reaches a maximum equal to 32.35 mg g^{-1} (CB) and 56.32 mg g^{-1} (CM) at a 100 ppm. This retention capacity is very important which show that this resin has a high affinity for lead. The comparative study of all experimental results has confirmed the bioadsorption potential of the studied bioadsorbent for the removal of the metal Pb(II).

Keywords: Lead ions Pb^{2+}; *Typha latifolia*; Adsorption; Fourier-transform infrared spectroscopy/scanning electron microscopy/energy-dispersive X-ray spectroscopy; Cellulose; Raw cellulose (CB)/modified cellulose; Kinetic modeling

1. Introduction

Water is essential to life on earth, but it is also essential to the industrial and agricultural development of human societies [1]. This accelerated development is often accompanied by atmospheric and water pollution, which poses a real problem for the environment. Industrial activity in the extraction or elaboration of metals generates aqueous effluents charged with toxic metallic elements in varying concentrations, and sometimes discharged without

* Corresponding author.

treatment into the receiving environment [2]. Thus, the pollution of water by heavy metals is currently a major concern for the quality of water and the environment [3]. This fact leads to the use of more suitable criteria for the protection of populations exposed to contamination by these metallic species, so it is important to look for severe means of treatment of industrial wastewater before its discharge into the natural environment [4,5].

The effluent treatment process aims to reduce the pollutant load to a level deemed acceptable for the receiving environment. Indeed, the processes implemented in conventional installations are generally expensive and consist of mechanical, biological or physical–chemical methods, such as precipitation, electrolysis, ion exchange, oxidation processes and adsorption.

Among these methods, adsorption is one of the most widely used processes in the world to reduce the concentration of metal ions in wastewater and drinking water systems [6,7].

Cellulose and its derivatives (chitin and chitosan), the main adsorbents used in water treatment, have many advantages, they allow the removal of a wide range of pollutants in different types of dyes, but also other organic and inorganic pollutants such as phenols, metal ions, pesticides, detergents etc. [8,9].

Adsorption is an effective technique used in the removal of dyes, odor, organic pollutants and inorganic heavy metal ions from industrial wastewater. Various absorbents are used in the adsorption process, including activated carbon, agricultural waste, chitosan and eucalyptus barks. Activated carbon is the most widely used adsorbent due to its excellent adsorption efficiency for organic and inorganic pollutants, but its use is inadequate due to its high cost. However, the fight against metal pollution has stimulated the search for clean technologies and especially processes using natural carriers and less cost for the removal of heavy metals from the Wastewater industry. Several studies have recently been developed for the elimination of heavy metals by plants [8].

Typha latifolia or reed fiber is a cosmopolitan plant, which can provide reliable aerobic treatment, reliable aerobic treatment. In recent decades, a lot of research has led to the development of this natural material in different fields such as an additive for building materials, the production of bioenergy [10], heavy metal phytoremediation [11].

In this context, the present investigative study the adsorption efficiency of two cellulose-based prepared materials CB and CM for the metal cation Pb(II) from contaminated solution. Initially, the parametric study was carried out through several parameters. Similarly, the thermodynamic parameters were calculated using Van't Hoff curves. Many kinetic models and adsorption isotherms have been tested to describe the adsorption mechanism [10].

2. Materials and methods

2.1. Extraction of microfibers

Traditional chemical treatments were used to adsorb the cellulose, with modifications to the waxing, alkali, and bleaching processes. The following is a description of the chlorine-free adsorption technique:

2.1.1. Waxing

Approximately 20 g of powder were waxed in a Soxhlet reflux with a 2/1 mixture of two products (acetone/ethanol) at 63°C for about 7 h; the goal of this step is to remove waxes and the adsorbate. The sample was then placed in a Buchner and dried under vacuum at room temperature for 3 h to remove any remaining solvents [11].

2.1.2. Alkaline treatment

The alkaline process was perfected to purify cellulose of reed fibers by removing lignin and hemicellulose. The adsorption-free mode was treated with an alkaline solution (7% NaOH by weight) with a 10/1 solvent/cellulose ratio at 80°C for 3 h with mechanical stirring. This technique was perfected three times, with the cellulose being filtered and washed with distilled water after each treatment to bring it up to pH [12].

2.1.3. Bleaching of cellulose

A subsequent bleaching procedure was used to remove any remaining lignin and bleach the cellulose fibers. The material was immersed in an 11% hydrogen peroxide solution, the pH was adjusted to 11 using 7% NaOH, and the system was rapidly agitated at 45°C for 3 h. The bleaching process was repeated again under the same conditions for more effective discoloration (Fig. 1), and the microfibers were filtered and rinsed with distilled water after each treatment [13].

2.1.4. Preparation of the biosorbent

To study the retention of lead ions by adsorption on cellulose (CB) and oxidized cellulose (CM), we prepared different masses in (g) of cellulosic materials (0.02, 0.05, 0.08, 0.1, 0.2, 0.3, and 0.5) using a balance. Our experimental work plan was as follows:

Study of the influence of certain physical-chemical parameters such as contact time, pH, initial concentration and the nature of the chemical pre-treatment applied to the support, in the Pb(II) retention process, varying only one parameter at a time, keeping the others constant; Determination of the nature of the adsorption isotherm; Determination of the adsorption kinetics.

Solubility in water 0.2, loss of mass 6% for T = 105°C and pH = 5–7.5.

The mass 0.1 g of cellulose was chosen in such a way that the complexation of the appropriate metal was sufficient.

2.2. Preparation of a metal cation solution

In our adsorption tests, we prepared stock solutions of Pb^{2+} ions using lead nitrate $Pb(NO_3)_2$ with a molar mass of 331.2 g mol^{-1}, The concentrations of the ions varied between 10 and 100 ppm.

The pH of the solutions was adjusted with NaOH or HNO_3. All solutions were prepared from analytical grade products and distilled water.

Solutions with lower concentrations are obtained by diluting this stock solution or an already diluted solution.

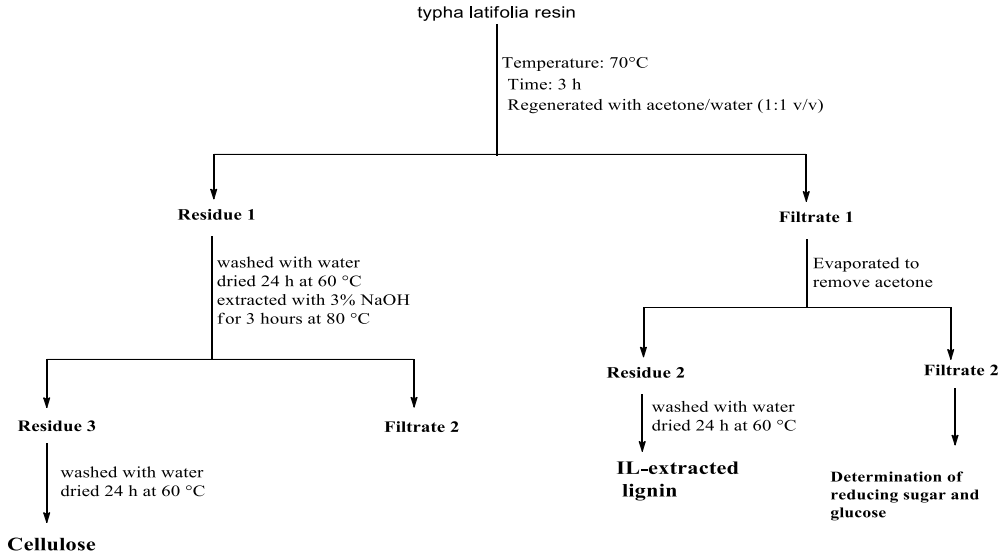

Fig. 1. Strategy for extracting cellulose from reed fiber.

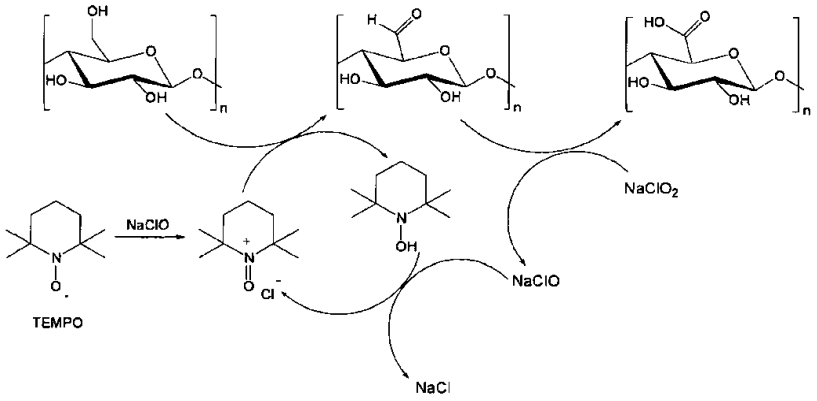

Fig. 2. Direct oxidation of cellulose.

2.3. Treatment of cellulose

However, the use of cellulose as a filter medium or adsorbent in wastewater treatment requires knowledge of the structure and texture of the material. This objective can be achieved in several ways, by increasing its specific surface. Depending on the type of treatment, these actions can be combined. However, the main constraints of chemical treatment are to avoid the loss or degradation of materials and to limit the formation of inhibiting products. In this context, and because of the economic and environmental importance of cellulose recovery in wastewater treatment, we were interested, first of all, in the question of the effect of chemical modification on the microstructure of cellulose within the framework of the formulation of cellulosic adsorbent materials.

The method described in the literature. Allowing the oxidation of cellulose was adapted for bark. Three grams of the crude cellulose is suspended in 300 mL of an aqueous solution containing 37 mg TEMPO (0.24 mmol), and 5.64 mL sodium hypochlorite (7.26 mmol) are represented in Fig. 2. The pH is adjusted and maintained at 10 by adding 0.1 M sodium hydroxide, when the pH stabilizes; the solution is neutralized by adding 0.1 M hydrochloric acid. The mixture is then kept at room temperature under magnetic stirring for 85 h. The cellulose is then rinsed with 1 L of ultrapure water and dried in a ventilated oven at 40°C before being weighed to obtain the mass yield of the reaction [15].

It has recently been shown that CM carboxyl groups can be introduced, resulting in a more increased surface charge compared to the hydrolysis of CB, in addition to the hydrolysis of HCl. TEMPO selectively oxidizes primary hydroxyl groups (C_6) to carboxylates, while secondary hydroxyl groups are unaffected [16].

2.4. Chemical analysis

2.4.1. X-ray diffraction analysis

The crystallinity of cellulose microfibers was investigated by X-ray diffraction (XRD) analysis, using a powder X-ray diffractometer (D8 ADVANCE A25 Bruker AXS GmbH, Germany) with Cu Kα radiation (1.5406 Å) at 40 kV

and 25 mA, in the range of 2θ = 5°–60° at a scanning rate of 0.02°s^{-1}. The crystallinity index (CrI) was calculated according to Segal equation:

$$\mathrm{CrI} = 100 \times \frac{\left(I_{200} - I_{\mathrm{am}}\right)}{I_{200}} \quad (1)$$

where I_{200} is the diffraction intensity at 2θ = 22°–23° and I_{am} is the minimum diffraction intensity at 2θ = 18°–20°.

The crystallite size was calculated as per the Scherrer equation:

$$L_{h,k,l} = 0.94 \times \lambda\beta\cos\left(\theta\right) \quad (2)$$

where λ is X-ray wavelength; β is the full width at half maximum in radians; and θ is the Bragg angle.

2.4.2. Morphological structure

A scanning electron microscope (SEM) (Quanta 250 FEG, FEI, USA) with an accelerating voltage of 15 kV was used to investigate the microstructure and the surface morphology of the obtained cellulose microfibers.

2.4.3. Thermogravimetric analysis

In order to study the thermal stability of the extracted cellulose microfibers, thermogravimetric analysis (TGA) was performed using a Mettler Toledo TGA/DSC instrument.

The scan was carried out from 30°C to 800°C at a heating rate of 10°C/min and under nitrogen atmosphere.

2.4.4. Fourier-transform infrared spectroscopy

To analyze the chemical changes of the samples and investigate functional groups in the extracted cellulose we used Fourier-transform infrared spectroscopy. The Fourier-transform infrared spectroscopy (FTIR) spectra were recorded on a Cary 660 FTIR Spectrometer (Agilent Technologies, USA) in a wavelength range of 4,000–400 cm^{-1} with a resolution of 4 cm^{-1}.

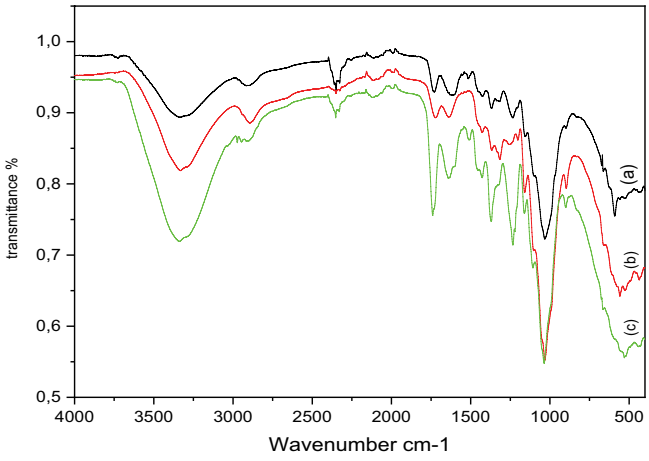

Fig. 3. FTIR spectrum of raw fiber (a), extracted cellulose (b) and oxidized cellulose (c).

2.5. Adsorption process

The liquid–solid adsorption of Pb(II) is performed in 250 mL beakers. A well-defined volume of the solution of the element to be adsorbed (100 mL) puts in contact with a quantity of the cellulose resin (0.1 g) for the time necessary to reach equilibrium under fixed conditions. At the end of the adsorption, the two phases, liquid and solid. An AA240FS variable atomic absorption spectrometer is used to test lead concentrations (AAS).

Adsorption (liquid–solid) is a process of transferring a solute (material) from a liquid phase to a solid phase. The time of intimate contact between the two phases is a limiting factor. The search for the time after which the bioadsorption equilibrium is reached is necessary. In this work, the study of this parameter is carried out at times ranging from 5 to 180 min. The results obtained are summarized in this chapter, while the calculation of the adsorption yield and the adsorption capacity is carried out by the respective use of the following relations [14–16].

$$\%\ \mathrm{Removal} = \frac{\left(C_0 - C_f\right)}{C_0} \times 100 \quad (3)$$

$$Q = \left(C_0 - C_f\right) \times \frac{v}{m} \quad (4)$$

where C_0 and C_f are respectively the concentrations of Pb(II) ions in the aqueous phase at the initial state, and at equilibrium in mol L^{-1}, V is the volume of the treated lead solution (100 mL) and m is the mass of the cellulose used (0.1 g).

3. Results and discussions

3.1. FTIR spectroscopic analysis

We used FTIR to investigate the chemical changes in the various materials explored and the functional groups in the isolated cellulose (FTIR spectra) are represented in Fig. 3.

The characteristic vibration bands were assigned, mainly in agreement with literature data, and taking into consideration the main differences between the infrared spectra of the material before and after treatment. It is evident that the formation of carboxylic groups of CM and hydroxyl groups of cellulosic chains. As shown in the FTIR spectrum, the characteristic peaks at about 1,233; 1,367; 1,733; 2,894 and 3,336 cm^{-1} are attributed to (C–O) stretching, (CH_2) symmetric bending, (C–H) stretching, and (O–H) stretching of cellulose, respectively. It is reported that the characteristic peaks of carboxyl groups in CM are located at about 1,733 cm^{-1} (C=O) and 1,280 cm^{-1} (C=O), while the peak of carbonyl groups in acids emerges at, on the other hand, the as-created polymeric network can surround and immobilize (Fig. 4C) and thus, a durable hydrophobic fabric filter can be obtained [17–20].

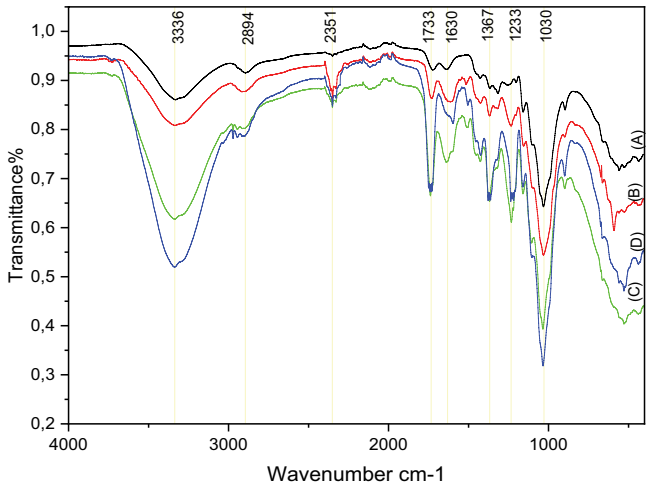

Fig. 4. FTIR spectra of cellulose brute (A), Pb(II) adsorbed before (B), and after cellulose extraction (C) and oxidized cellulose (D).

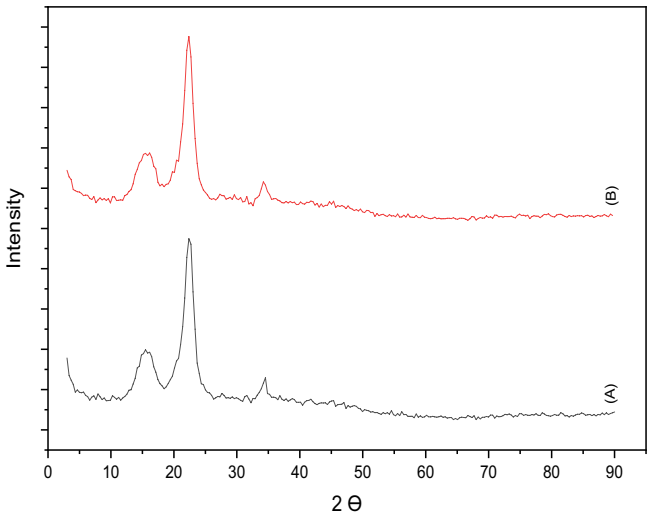

Fig. 5. Diffractogram of commercial microcrystalline cellulose (a) and reed filter extract (b).

Infrared analysis (FTIR) of the cellulosic compounds after processing shows the presence of functions characteristic of these coupling agents. The peaks at 1,733 and 1,630 cm^{-1} are respectively characteristics of the carbonyl functions and the conjugated double bonds. These two functions should normally be present in the compounds after grafting. The intensity of the absorption band at 1,662 cm^{-1} is more intense than that at 1,726 cm^{-1} and the peaks are separated by 64 cm^{-1}. In α, β-unsaturated compounds, the vibrational frequency of the carbonyl bond are lowered from 15 to 40 cm^{-1}. It is also noteworthy that the spectra of the carbonyl compounds show slightly lower values for the C=O bond elongation vibrational frequencies when obtained in the solid state compared to those in dilute solutions. This suggests the presence of anhydride on the surface and therefore that not all reactive sites were consumed during the grafting reaction. In addition, the band at 893 cm^{-1} characterizes the isolated aromatic hydrogen in the modified fiber [18].

3.2. XRD analysis

X-ray diffraction is used to study the crystal structure of commercial microcrystalline cellulose and reed filter plant extract. They are shown in Fig. 5.

The XRD spectrum of cellulose and reed extract shows three lines located at 2θ = 16.57°–16.50°, 22.81°–22.40° and 34.77°–34.79°, respectively. The line at 2θ = 16.57°–16.50° corresponds to the diffraction of the (110) type I crystalline cellulose plane, the lines at 2θ = 22.81°–22.40° and 34.77°–34.79° correspond to the diffraction of the (002) and (004) planes at the same crystal form. The reed adsorbed therefore contains crystalline type I cellulose in the form of elongated crystals, as the (004) band is much finer than the other lines [19].

For comparison, the crystalline adsorbed portion of the reed filter shows strong structural analogies with commercial microcrystalline cellulose. On the other hand, microcrystalline cellulose has a higher degree of crystallinity because the amorphous contribution (30°) is greater in the reed adsorbed [20].

3.3. Thermogravimetric analysis

The thermal stability of the cellulose and filter adsorbed was studied by gravimetric analysis at a temperature rise of 10°C/min. The percentage mass change of the sample as well as its derivative with respect to temperature is expressed as a function of temperature from 30°C to 800°C, is represented in Fig. 6.

Two thermal events are notable. The first mass loss of cellulose, which is about 100°C, is attributed to water loss. The water content of cellulose is estimated at 4.6%. This rate varies with the relative humidity of the ambient air.

The second event is highlighted in the temperature window 250°C–450°C. Then the thermal degradation of the polysaccharide is observed. The maximum of the derived peak at 318°C and its narrow shape reflects the degradation of the pure material. At temperatures above 800°C, the residues represent about 0.7%.

The thermal stability of a pure material, such as cellulose, can be affected by morphology or sampling. The same type of analysis is performed with reed extract. The water content of the extract is estimated to be 5.5%. Maximum derivation peak at 300.33°C. At temperatures above 800°C, the residues represent about 1.8%.

A comparison of these two thermograms shows that the behavior is slightly different. This may be due to the difference in crystallinity and/or grain size of the red filter.

3.4. Morphological properties of chemically purified cellulose microfibers

The fiber/matrix interface in the composites was studied by SEM by observing the fracture region of the specimens (Fig. 7). The appearance of the different surfaces is relatively close together, chemical variations seem to have little effect on the surface. Indeed, the various fiber/matrix interfaces are quite fragile as shown by the appearance of certain voids due to the stretching and tearing of the fibers. We can also see that, in images 7a and 7c, fault zones have fewer defects [21]. Modified cellulose

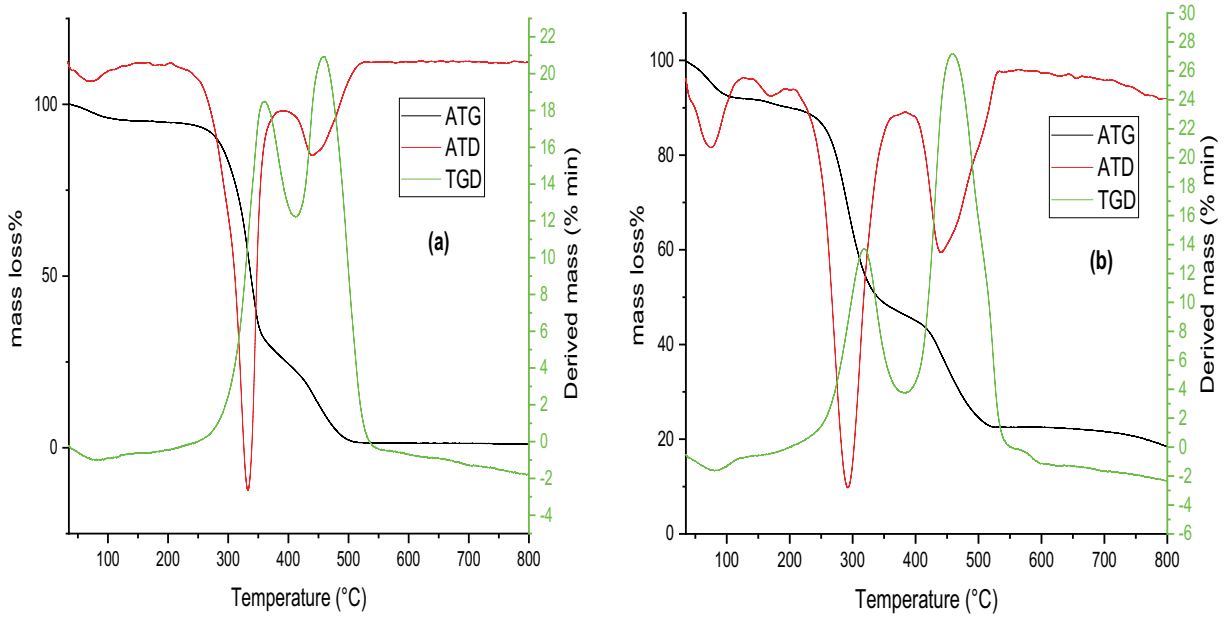

Fig. 6. ATG, ATD, TGD thermogram of commercial microcrystalline cellulose (a) and reed filter adsorbed (b).

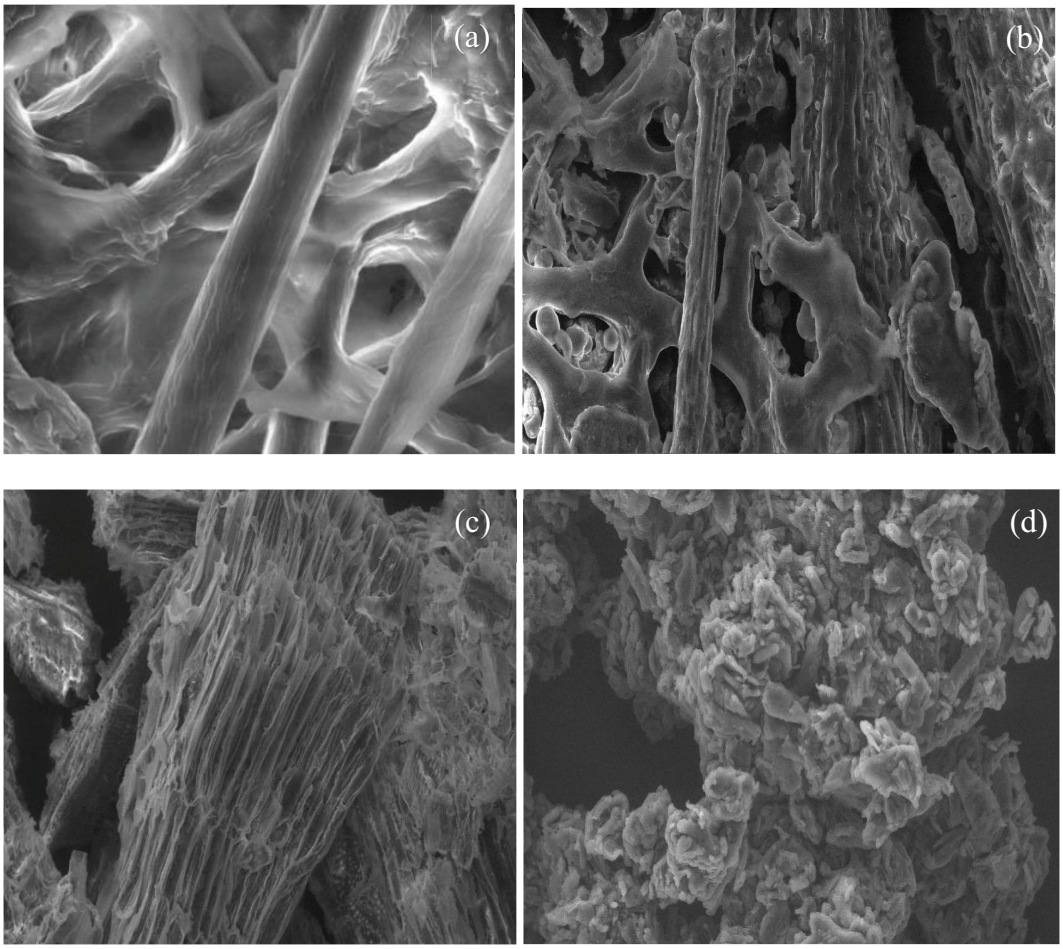

Fig. 7. SEM images of cellulose (a,b) microfibers extracted from reed plant filter and their oxidation (c,d) before and after Pb(II) extraction.

appears to have more affinity than unmodified cellulose. This is explained by the higher FTIR for the oxidation reaction of cellulose, therefore more hydrophobic/hydrophobic interactions. Chemical changes cause a decrease in surface energy. However, the absence of strong bonds between the modified fibers and the cellulosic substrate leads to proximal behaviors, observed that the oxidized cellulose was very well dispersed in the cellulosic substrate. Before and after modification were well separated from each other and no major aggregate was observed, resulting in a relatively homogeneous material [17]. In addition, no deterioration was observed after adsorption, which confirms that the treatment developed preserves the integrity of the fibers. It was found that the oxidized cellulose was very well dispersed in the cellulosic matrix.

3.5. Adsorption studies

3.5.1. Effect of contact time

The kinetic study corresponds to the determination of the sufficient and necessary time to reach the equilibrium or the maximum adsorption. To do this, we take a beaker into which we introduce a quantity of 0.1 g of cellulose resin and 100 mL of a 10 ppm lead solution. The beaker is shaken for a determined and different period of time (from 5 to 180 min). After separation of the two phases, the Pb(II) content in the aqueous phase is analyzed by ICP.

From Fig. 8, it can be seen that the extraction kinetics is fast, the equilibrium time is reached after 90 min for CB and 60 min for CM. Under the operating conditions adopted for this study, it can be seen that the retention efficiency of Pb^{2+} ions is 66% for CB and 98% of CM and that the sorption capacity is around 6.48 mg and 9.85 mg of Pb(II) per 1 g of CB and CM support respective, the curves can be divided into three steps:

During the first one (from t = 0 to 20 min), The adsorption rate is very fast, (the adsorption yield of CB and CM increases from 0% to 47.9%; and from 0% to 65.8%, and the adsorption capacity increases from 0% to 5.58 mg g^{-1} and from 0% to 6.54 mg g^{-1}) [26].

This behavior can be explained by:

The availability of a large number of active sites on the resin for the retention of free Pb^{2+} in solution, the presence of a more lead-rich aqueous phase.

During the second stage (t from 20 to 80 min for CB), (t from 20 to 60 min for CM) the extraction rate slightly decreases (the adsorption yield of CB and CM goes from 47.9% to 64.6%; and from 65.8% to 87.43% and the sorption capacity goes from 5.58 to 6.48 mg g^{-1}; and from 6.54 to 8.74 mg g^{-1}).

This behavior can be explained by:

With the progress of the adsorption (increase of time), the active sites for the support become more and more unavailable (saturations). The aqueous phase is more and more depleted in the lead.

During the third stage ($t \geq 80$ min. CB), ($t \geq 60$ min. CM), the adsorption rate cancels and equilibrium are reached.

This behavior can be explained by the saturation of our support and the equality between the number of moles of lead that passes from the aqueous phase to the solid phase (adsorption) [27].

3.5.2. Effect of pH

In beakers, 100 mL of the aqueous solution of lead of concentration 10 ppm is introduced and the pH is adjusted by the addition of a nitric acid solution (HNO_3) or an aqueous solution of sodium hydroxide (NaOH). Measured amounts of acid or base solution are added so that the concentration of Pb(II) is the same in all beakers. About 0.1 g of the cellulose is introduced into each beaker.

The two phases are stir for 180 min. Afterwards, the two phases are separated and samples are taken for quantitative analysis of Pb(II) with AAS.

The pH of the aqueous phase is an important factor in controlling the movement of a positively charged particle from one phase to another. The pH can act simultaneously

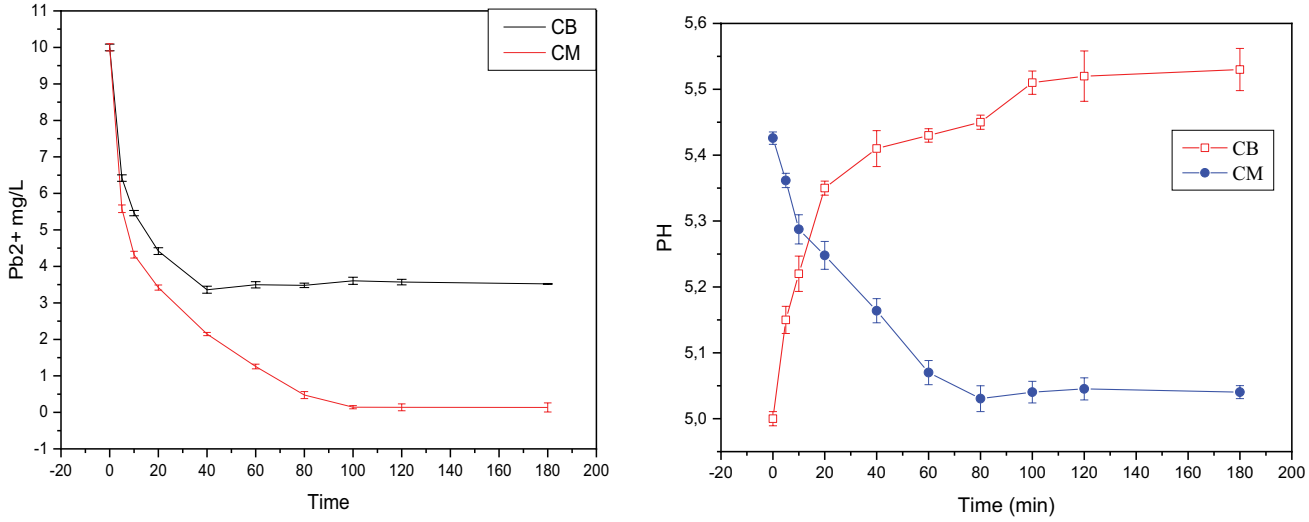

Fig. 8. Effect of stirring time on [Pb^{2+}] and pH of Pb(II) by CB and CM resin.

on the predominance of Pb(II) species present in solution and on the acidic or basic form of our support. The study of the effect of the initial pH on the adsorption of Pb(II) was performed by adsorption at pH [28].

Fig. 9 shows that the yield of Pb^{2+} adsorption by the cellulose resin is low (slow reacting) in the pH range (6,8), then it increases rapidly in the pH range (4–5.5), then stabilizes and becomes almost constant, at a maximum equal to 65.8% for CB and 98.6 for CM, at a pH between 5.5 and 6.5. These findings can be attributed either to the behavior of the adsorbent with respect to the change of pH in the aqueous phase or to the behavior of the Pb(II) cations (appearance and/or disappearance of Pb(II) species in the aqueous phase) at different pH [29].

3.5.3. Effect of lead concentration

Masses of the 0.1 g resin are introduced into beakers to which equal volumes (100 mL) of lead solutions of different concentrations have been added. The mixtures are stir for 180 min. After separation of the two phases, the Pb(II) content in the aqueous phase is analyzed by AAS [16].

The influence of the initial Pb(II) concentration on the adsorption yield and the adsorption capacity was studied by varying the Pb(II) concentrations in the aqueous phase from 10 to 100 ppm. The results obtained (adsorption yield and adsorption capacity) are shown in Figs. 10 and 11.

Fig. 10 shows that the CB and CM adsorption yield respectively, decreases with increasing Pb(II) concentration and reaches a minimum value of 32.35% and 56.32% for a Pb(II) concentration of 100 ppm. For [Pb(II)] concentrations <100 ppm the yield increased from 32.35% to 66.17% and from 56.32% to 98.8% when the lead concentration becomes equal to 10 ppm.

Fig. 11, shows that the sorption capacity increases with increasing initial lead concentration and reaches a maximum equal to 32. 35 mg g^{-1} of (CB) and 56.32 mg g^{-1} of (CM) at a concentration greater than or equal to 100 ppm. This increase is due to the increase in the number of lead ions in the aqueous phase, which pushes the adsorption equilibrium towards the formation of more lead complexes in the solid phase [31].

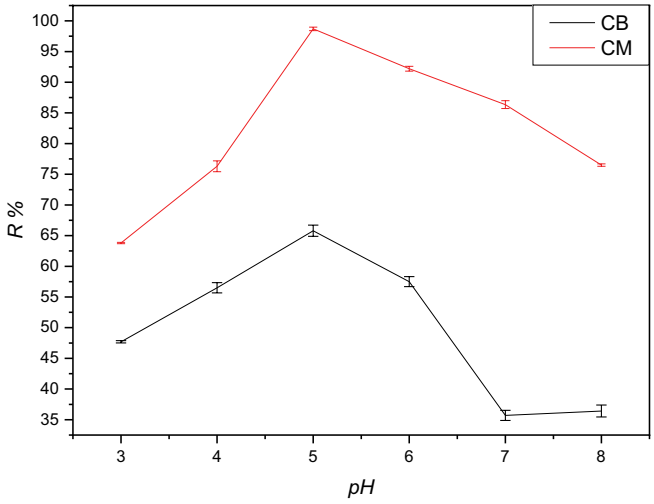

Fig. 9. Effect of initial pH on the adsorption efficiency of Pb(II) by CB and CM.

3.5.4. Mass effect

The aim of this study is to determine the dry quantity that will allow purifying a given volume of lead solution. The study was carried out with dry masses ranging from 0.02 to 0.8 g, each of which was placed in a metallic solution at 10 ppm and pH = 5, the system was agitated at room temperature for 180 min. After the separation of the two phases, the Pb(II) content in the aqueous phase was analyzed by AAS.

The curves representing the variations of the percentage of lead eliminated as a function of the mass of cellulose powder are represented in Fig. 12.

The removal efficiency of metal ion could be higher with the increase of adsorbent mass, in general, a large amount

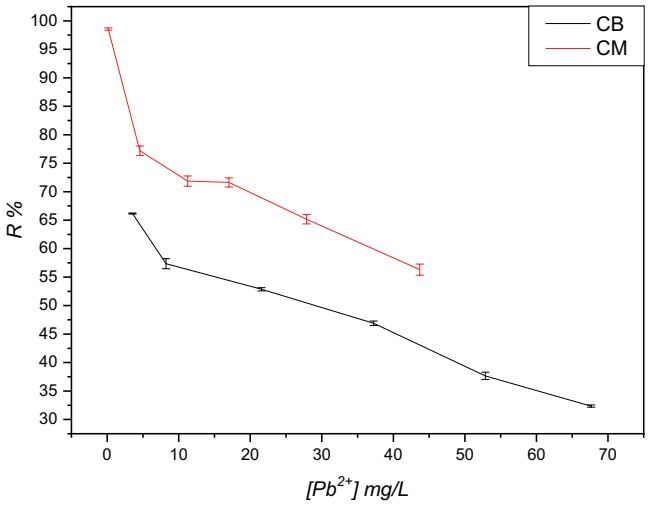

Fig. 10. Effect of initial Pb(II) concentration on adsorption yield by CB and CM.

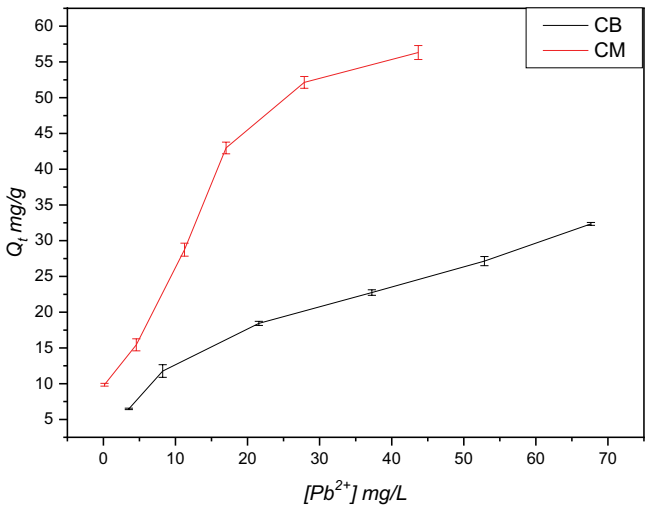

Fig. 11. Effect of initial Pb(II) concentration on sorption capacity.

of adsorbent in the adsorption process could guarantee the availability of more adsorption sites, which contributes to high adsorption capacity, moreover, the removal efficiency as a function of adsorbent mass varied significantly with each mass [32]. According to this study, a mass of 0.1 g in BC allows the removal of more than 68% of the lead, with 0.2 to 0.5 g the removal rate rises to 97%. And 0.1 g in CM allows eliminating more than 98% of the lead.

3.5.5. Effect of temperature

In five beakers, containing 100 mL of the 10 ppm lead solution and 0.1 g of the cellulose. Each mixture is stirred in a water bath of fixed temperature (25°C, 35°C, 45°C, 55°C and 65°C) on a magnetic stirrer equipped with a temperature controller for 90 min. Once equilibrium is reached, the two phases are separated and the Pb(II) content in the aqueous phase is analyzed by AAS.

The removal efficiency of metal ions increases with temperature, indicating that the adsorption process is endothermic for BC. The molecular motion in the adsorption process could be accelerated at higher temperature; therefore, the adsorption equilibrium time could be reduced. In addition, the CM undergoes a decrease in efficiency as a function of temperature due to the loss of mass of the CM modified in high temperature [33].

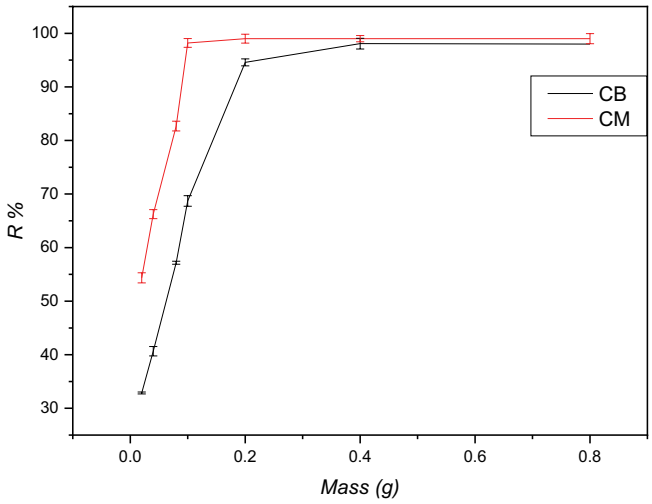

Fig. 12. Effect of mass on the extraction efficiency of Pb(II) by CB and CM.

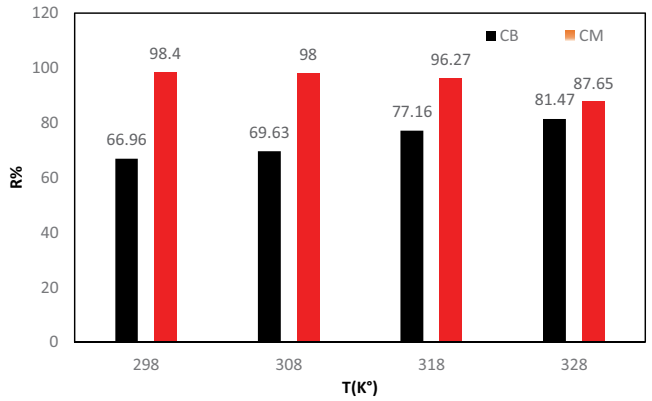

Fig. 13. Effect of temperature on the extraction efficiency of Pb(II) by CB, CM.

3.6. Adsorption isotherms

The model of adsorption equilibrium consists in representing, by mathematical laws, the equilibrium relationship between the quantity of pollutant in the liquid phase (C_e) and that adsorbed on the material (Q_e). In this study, the adsorption equilibrium is analyzed by applying the Langmuir and Freundlich models which are commonly used by researchers to study the adsorption isotherms of adsorbent/adsorbate systems.

3.6.1. Langmuir isotherm

The Langmuir isotherm theory assumes that adsorption is monolayer and takes place at specific homogeneous sites of the adsorbent [34]. The results of the Pb(II) ion adsorption tests on wood ash were treated by the Langmuir model represented by the following equation:

$$\frac{C_e}{Q_e} = \frac{1}{Q_{\max} \cdot K_l} + \frac{C_e}{Q_{\max}} \tag{5}$$

where C_e is the equilibrium concentration (mg L^{-1}), Q_e is the equilibrium adsorbed quantity (mg g^{-1}), K_l is the equilibrium constant relative to the Langmuir model, and $Q_{\max}$ is the maximum adsorbed quantity (mg g^{-1}). The values of $Q_{\max}$ and K_l are determined from the intersection with the y-axis and the slope of the line $C_e/Q_e = f(C_e)$ (Fig. 14).

The results obtained show that the correlation coefficient (R^2 = 0.9972 and R^2 = 0.9197) of the Langmuir model is very close to unity (Table 1). The use of the linear regression line [Eq. (3)] allowed us to determine the maximum adsorption

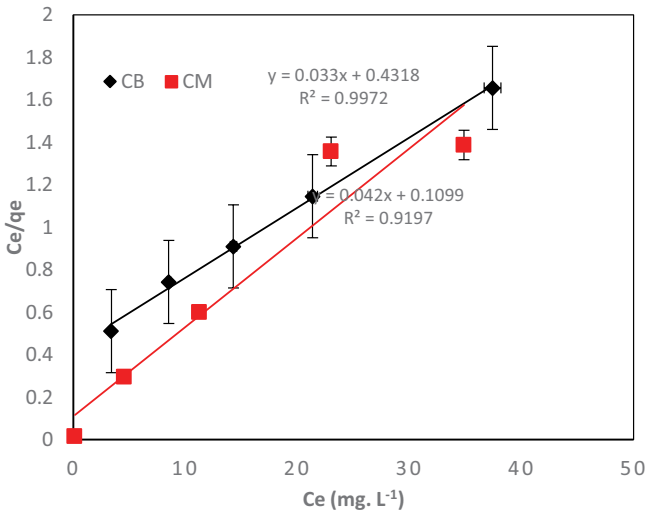

Fig. 14. Linear form of the Langmuir model of Pb(II) on the two cellulose fibers.

Table 1
Adsorption parameters of Pb(II) ion on raw and modified cellulose fiber according to Langmuir and Freundlich models

Isotherms	Constants	CB	CM
Freundlich	K_f (mg^{1-n} L^n g^{-1})	2.645	1.38
	n_F	0.930	0.210
	R^2	0.979	0.772
Langmuir	q_m (mg g^{-1})	30.300	43.80
	K_l (L mg^{-1})	0.076	0.380
	R^2	0.997	0.920

capacity Q_{max} and the Langmuir adsorption equilibrium constant.

An essential characteristic of the Langmuir isotherm can be expressed in terms of a dimensionless constant called the separation factor, defined by the Eq. (6):

$$R_l = \frac{1}{1 + K_l C_0} \tag{6}$$

where C_0 is the initial concentration of the adsorbate (mg L^{-1}) and K_l is the Langmuir constant (L mg^{-1}). A separation factor $R_l > 1$ indicates that adsorption is unfavorable, if $R_l = 1$ adsorption is said to be linear, adsorption is said to be favorable when $0 < R_l < 1$, and a zero separation factor ($R_l = 0$) indicates that adsorption is irreversible [35]. In our case, the R_l values found are all between 0 and 1, which indicates favorable adsorption.

3.6.2. Freundlich isotherm

The Freundlich isotherm assumes that the adsorption is multilayered and that the surface of the adsorbent is heterogeneous. It can be expressed by the following relationship:

$$\ln Q_e = \ln K_f + \frac{1}{n} \ln C_e \tag{7}$$

The plot of $\ln(Q_e)$ vs. $\ln(C_e)$ for the adsorption of methylene blue on wood ash is a straight line with a slope of $1/n$ and an intercept of $\ln(K_f)$ (Fig. 15). The value of $1/n$ gives an indication of the validity of the adsorption of the adsorbent–adsorbate system. A value of $1/n$ between 0 and 1 indicates favorable adsorption [36]. The numerical values of K_f and $1/n$ calculated respectively, from the intersection with the intercept and the slope of the isotherm line, are shown in Table 2.

The numerical value of $1/n = 0.75$ and 0.71 indicates that the adsorption is favorable. The correlation coefficient R^2 is 0.97 and 0.77, which is lower than that of the Langmuir model (R^2 = 0.98 and 0.91). This indicates that the adsorption of Pb(II) ion on crude and modified cellulose fiber follows the Langmuir model as well as the Freundlich model [36].

As shown in Table 1, the Langmuir isotherm corresponds fairly well to the experimental data ($R^2 > 0.98$ of CB and $R^2 > 0.92$ of CM). The monolayer adsorption capacity conformity to this model [51] was 30.300 mg g^{-1} for the CB and 43.80 mg g^{-1} for CM.

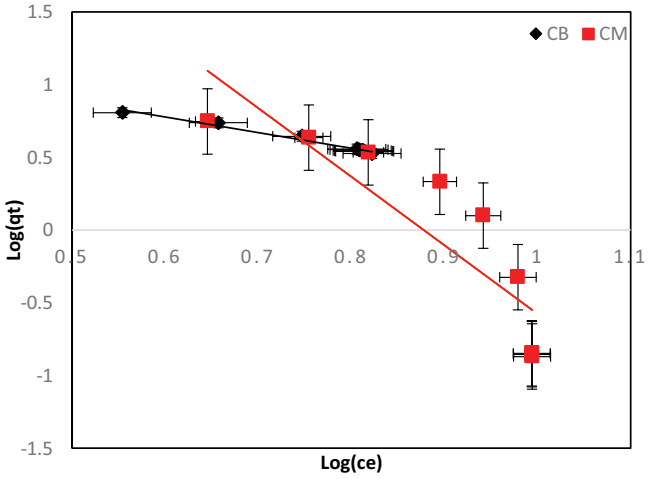

Fig. 15. Linear form of the Freundlich model of Pb(II) on the two cellulose fibers.

Table 2
Kinetic parameters relating to the adsorption of Pb(II) ion on the two cellulose fibers

Model	Constants	CB	CM
Pseudo-first-order	k_1 (min^{-1})	0.0072	0.027
	Q_e (mg g^{-1})	1.36	1.46
	R^2	0.60	0.89
Pseudo-second-order	k_2 (g mg^{-1} min^{-1})	0.23	0.1
	Q_e (mg g^{-1})	6.61	9.50
	R^2	1.00	0.998

3.7. Kinetic adsorption models

Two kinetic models were studied; their parameters and Pb(II) correlation coefficients were calculated from Figs. 16 and 17 and listed in Table 3.

3.7.1. Pseudo-first-order kinetics model (Lagergren model)

The thermodynamic equilibrium between the adsorbent in the liquid phase and the adsorbate fixed on the solid is achieved at a rate that is dependent not only on the rate at which the constituents diffuse in the adsorbent and in the fluid, but also on the adsorbent–adsorbate interaction.

The time is dependent analysis of a compound adsorption on an adsorbent allows us to investigate the impact of contact time on retention. For this goal, two models were used to explain the mechanism of Pb(II) ion adsorption kinetics of cellulose and its derivatives:

$$\log\left(q_e - q_t\right) = \log\left(q_e\right) - \left(k \cdot \frac{1}{2.303}\right) t \tag{8}$$

where k (L min^{-1}): adsorption rate constant of the pseudo-first-order kinetics [37].

Fig. 16 shows the results of the application of the pseudo-second-order kinetic model for the adsorption of Pb(II) ion by the two cellulose fibers. The calculated values of the adsorbed quantities Q_e, the pseudo-second-order constants k_2 and the regression coefficients R^2 are given in Table 2. From these results, it appears that the R^2 values are very high and are all in the order of 0.99 and far exceed those obtained with the pseudo-first-order model. The quantities fixed at equilibrium Q_e are very close to the values found experimentally. These last two observations lead us to believe that the adsorption process follows the pseudo-second-order model.

3.7.2. Pseudo-second-order kinetics model

The design of a batch bioadsorption system requires information on the adsorption mechanism. Adsorption kinetics are necessary to determine the adsorption rate. Two kinetic models, including pseudo-first-order and pseudo-second-order Lagergren kinetic models, were tested to match the experimental kinetic data. Following Eqs. (5) and (6) for the expression of pseudo-first-order and second-order kinetic models respectively.

$$\frac{t}{q_t} = \frac{1}{\left(K_2 \cdot q_e^2\right)} + \left(\frac{1}{q_e}\right) \tag{9}$$

With k_2 (g mg^{-1} min^{-1}): adsorption rate constant of the pseudo-second-order kinetics [33].

From Fig. 16 it is observed that for the first order kinetic model, the correlation coefficient R^2 = 0.9992 and R^2 = 0.998 for the cellulosic fiber, the adsorption capacity is much lower than that obtained experimentally. On the other hand, the correlation coefficient for the second-order kinetic model is shown in Fig. 17, and the values obtained are comparable to the experimental values. This observation suggests the applicability of the second-order kinetic model on the adsorption process in this study [39].

The value of the R^2 correlation coefficient determined using the so-called second-order equation was closer to unity than the first order equation for all of the first concentrations studied.

Similarly, the difference between the predicted ($Q_{e\text{-cal}}$) and empirically determined ($Q_{e\text{-exp}}$) for the said second line is relatively minor compared to that estimated for the said first line, which is far from the experimental adsorption capacity [40].

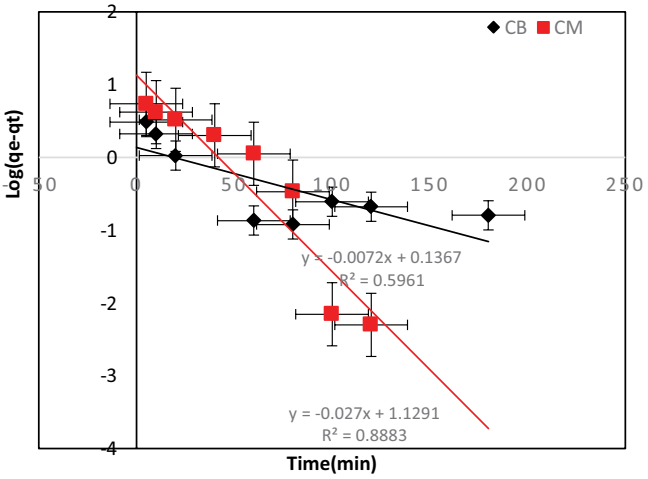

Fig. 16. Model of the pseudo-first-order kinetics of adsorbed Pb(II).

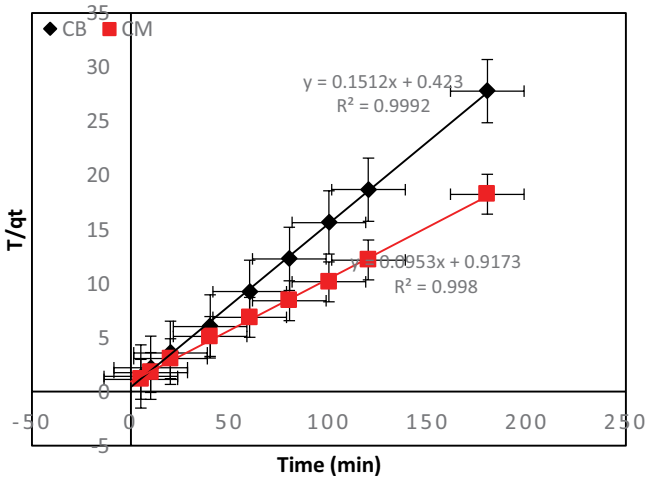

Fig. 17. Model of the pseudo-second-order kinetics of adsorbed Pb(II).

Table 3
Thermodynamic parameters for Pb(II) ion adsorption on the two cellulose fibers

	T (K)	lnK_D (L g^{-1})	$\Delta H°$ (kJ mol^{-1})	$\Delta S°$ (J mol^{-1} K^{-1})	$\Delta G°$ (kJ mol^{-1})
CB	298	0.31	9.52	34.30	–09.89
	308	0.36			–10.23
	318	0.53			–10.58
	328	0.64			–10.92
CM	298	1.79	–24.87	–67.62	–04.71
	308	1.69			–04.04
	318	1.41			–03.36
	328	0.85			–02.69

The physisorption, which encompasses the forces and electronic exchanges between the adsorbent and the adsorbate, is primarily responsible for the binding of Pb(II) ions to the investigated shells, according to a satisfactory fit of the experimental results and linear regression to the pseudo-second-order model [41].

3.8. Thermodynamic parameters

The thermodynamic parameters of lead on the cellulose surface were determined at different temperatures with an initial Pb^{2+} concentration of 20 mg L^{-1} using the following equations [42]:

$$\Delta G_{ads} = \Delta H_{ads} - T\Delta S_{ads} \quad (10)$$

$$\Delta G_0 = -RT \cdot \ln K_c \quad (11)$$

where T is the temperature in degrees Kelvin, R (8.314 × 10^{-3} kJ mol^{-1} K^{-1}) is the perfect gas constant and K_c is the distribution coefficient determined as follows: $K_D = Q_e/C_e$.

With Q_e: adsorption capacity at equilibrium (mg g^{-1}); C_e: equilibrium concentration of the solute in solution (mg L^{-1}).

$\Delta H°$ and $\Delta S°$ are determined from the slope and intercept of the plot of $\ln(K_D)$ vs. $1/T$ using the following Van't Hoff equation [43]:

$$\log K_D = \frac{\Delta S°}{2.303 \times R} - \frac{\Delta H°}{2.303 \times RT} \quad (12)$$

$\Delta H°$ and $\Delta S°$ were calculated from the slope and intercept of the plot of $\ln(K_D)$ vs. $1/T$. Their values are shown in Table 3.

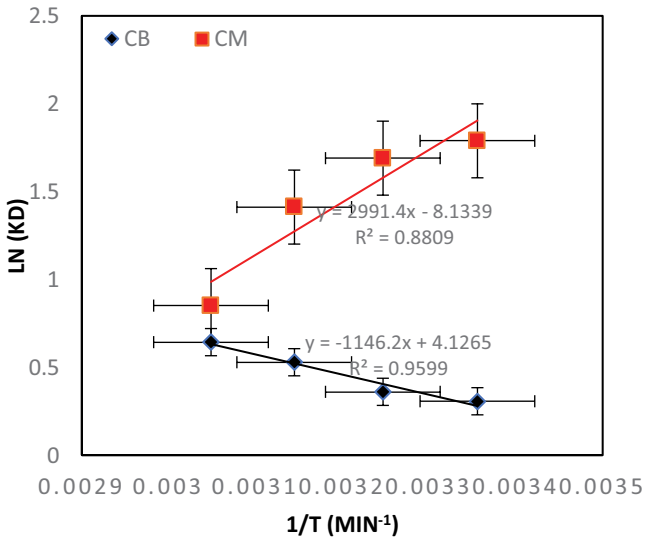

Fig. 18. Van't Hoff curve of Pb(II) adsorption on the two cellulose CB and CM.

The profile of the curve $\ln(K_D) = f(1/T)$ is a straight line, and is represented in Fig. 18 indicating that as the temperature rises, the breakdown becomes more prominent, resulting in higher molecular fluctuations and easy breaking of the hydrogen bond [44].

Table 3 lists the numerical values of the thermodynamic parameters. Negative $\Delta G°$ values show the spontaneity and feasibility of adsorption between the Pb molecules and the substance's surface with a high affinity [51]. Adsorption indicates that the support can withstand high temperatures. During adsorption, a positive value of $\Delta S°$ indicates increasing randomness at the surface. Furthermore, the positive value of $\Delta H°$ confirms that the adsorption of Pb(II) on the adsorbent is of this scale, demonstrating that physical adsorption is the primary adsorption mechanism of oyster meal [45].

- The positive values of enthalpy change ($\Delta H°$) underline the endothermic nature of the adsorption process [45] that is in agreement with the increase of adsorption capacity with increase of temperature. Its relative low value supports the statement that adsorption process occurs through a combination of physical van der Waals interactions and electrostatic attractions.
- The positive value of entropy change ($\Delta S°$) is characteristic to the increased randomness at the solid liquid interface during adsorption of heavy metal ions, indicating also some structural changes in both adsorbate and adsorbent [50,51].

3.9. Comparative studies on the adsorption of Pb(II) ions by cellulose and their derivatives

Some authors have focused on increasing the number of carboxylic acid functions, thus demonstrating a proportional relationship between their number and the quantity of ions fixed; this observation is valid when the adsorption is exclusively due to carboxylic acid functions and of the same acidity in the case of homogeneous materials such as cellulose. Table 4 gives some examples of modifications of natural polymers for use as adsorbents.

A review was devoted to the chemical modifications of cellulose and the resulting bioadsorbent. Esterification, halogenation, etherification and oxidation strategies were studied, most of which were transposed to bioadsorbent

Table 4
Examples of chemical modifications of some cellulose families for use as Pb(II) ion adsorbents

Adsorbent	Rendement en %	Reference
Cellulose–manganese oxide	80.00	[46]
Carboxymethylcellulose	70.00	[47]
H_2O-H_2SO_4-MSO_4 cellulose	99.00	[48]
Cellulose sulfonate	84.00	[49]
Typha latifolia	92.00	[50]
Remove the MO dye	80.20	[51]
Cellulose	68.00	This Works
Oxidized cellulose	97.00	This Works

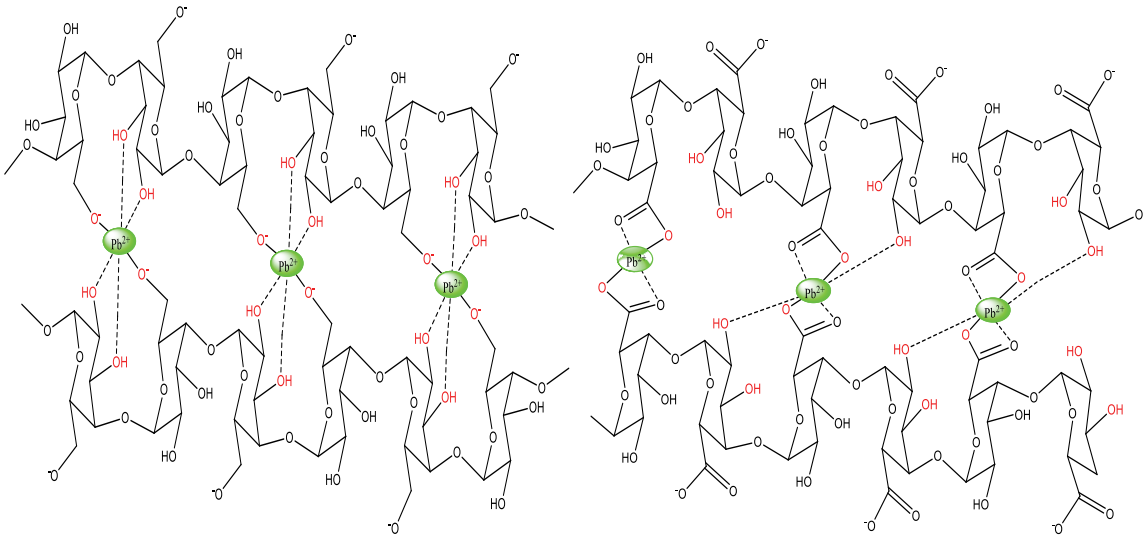

Fig. 19. Possible mechanisms of biosorption of Pb(II) by both types of extractant.

made up of various proportions of cellulose such as wood. Quantitatively, the adsorption results depend on the chemical modification carried out as well as on the metal considered. They are also difficult to compare because of the great variability of the experimental conditions between the different authors. The best retention capacities are obtained, in the case of Pb(II), following oxidized cellulose and sulfuric acid grafted onto cellulose.

3.10. Possible mechanisms of bioadsorption

Cellulose has different hydrogen bonding systems, which have an influence on the adsorption phenomenon, the reactivity of hydroxyl groups and the crystallinity of cellulose samples.

In this mechanism, Pb(II) adheres to the surface of CB and CM by ion-covalent bonds. Complexation (or chemisorption) is accompanied by a profound change in the electronic charge distribution of the adsorbed molecules and by the loss of at least one water molecule from the hydration sphere. Electrons are exchanged between the ions of the surface and the adsorbed Pb(II). The forces involved are of the same type as those involved in the formation of chemical bonds [22,24,25].

By studying the sorption of Pb^{2+} on our raw resin and modified showed that even in the presence of basic pH can be adsorbed for CM it concludes that the bonds are strong and that the mechanism involved and chemisorption and that the mechanism of complexation is always accompanied by an exchange of ions in this case Pb^{2+} reacts with carboxylic and/or hydroxyl groups present on the surface of CB and CM that in exchange release a proton H^+ is represented in Fig. 19. Cellulose also contains hydrophobic zones (around the carbon atoms) which have some influence on the overall properties, including solubility, the oxygen atoms of the D-glucopyranose ring and the glycosidic bond interact with each other within the chain or with another cellulose chain by forming intramolecular and intermolecular hydrogen bonds [23,30,38].

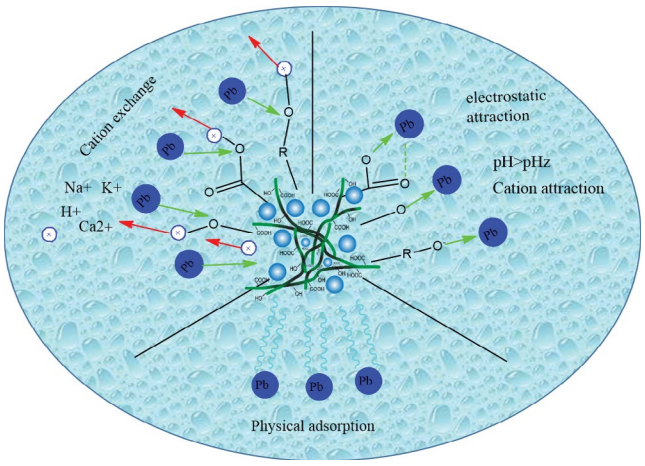

Fig. 20. Mechanisms ionic and electrostatic interaction.

The $^-$OH groups found in the cellulose and hemicellulose of reed filters, as well as the aromatic structures contained in the lignin, influences the biosorption process. Aromatic structures contained in the lignin, influence the biosorption process. The cationic characteristics of Pb(II), on the other hand, have been shown to delocalise the charge. They can be found in sulphate or nitrogen; however, they are more often found on nitrogen atoms. As the carboxyl groups groups are available for adsorption of charged Pb(II) at these pH values pH > PH_{ZC} values and biosorbent the surface is negatively charged due to the COO^- groups the optimum pH range for Pb(II) biosorption was 5.0 to 7.0, as shown in Fig. 20.

4. Conclusion

Current ecological concerns due to the large volumes of water used in industry as well as increasingly stringent discharge standards must find a suitable solution. The problems of discharges continent traces of heavy metals is

becoming more and more alarming and adequate solutions are increasingly sought.

The influence of initial metal ion concentration and temperature on the adsorption of Pb(II) from aqueous solution onto cellulose (CB) extracted from reed fibers and their cellulose-modified (CM) oxidation with the metal cation was examined. Batch experiments were carried out at pH 5.0 and an adsorbent dose of 10 mg L^{-1}, previously established as optimal, varying the initial concentration of Pb(II) between 10 and 100 mg L^{-1} and the temperature between 25°C and 65°C. Two isotherms (Langmuir and Freundlich) were applied to the equilibrium data and the fitted parameters were used to determine the thermodynamic parameters of the adsorption process. The adsorption equilibrium was well described by the Langmuir model. The maximum adsorption capacity of functionalized cellulose for Pb(II) ions increases slightly with increasing initial concentration from 32.35 mg g^{-1} for (CB) and 56.32 mg g^{-1} at (CB). Furthermore, thermodynamic studies indicate that the adsorption of Pb(II) onto biomass is an endothermic process for (CB) (ΔH°CB = 9.52 kJ mol^{-1}) and exothermic for (CM) (ΔH°CM = –24.87 kJ mol^{-1}) and spontaneous (ΔG°CB = –9.89, –10.92 kJ mol^{-1}) (ΔG°CM = –4.71, –2.69 kJ mol^{-1}) in the temperature range studied.

Refer ences

[1] D. Bulgariu, L. Bulgariu, Sorption of Pb(II) onto a mixture of algae waste biomass and anion exchanger resin in a packed-bed column, Bioresour. Technol., 129 (2013) 374–380.

[2] I.S. Bădescu, D. Bulgariu, I. Ahmad, L. Bulgariu, Valorisation possibilities of exhausted biosorbents loaded with metal ions – a review, J. Environ. Manage., 224 (2018) 288–297.

[3] A.M. Ghaedi, M. Ghaedi, A. Vafaei, N. Iravani, M. Keshavarz, M. Rad, I. Tyagi, S. Agarwal, V.K. Gupta, Adsorption of copper(II) using modified activated carbon prepared from Pomegranate wood: optimization by bee algorithm and response surface methodology, J. Mol. Liq., 206 (2015) 195–206.

[4] M.D. Meitei et M.N.V. Prasad, Adsorption of Cu(II), Mn(II) and Zn(II) by Spirodela polyrhiza (L.) Schleiden: Equilibrium, kinetic and thermodynamic studies, Ecol. Eng. 71 (2014) 308–317, doi: 10.1016/j.ecoleng.2014.07.036.

[5] S. Vasudevan, J. Lakshmi, G. Sozhan, Optimization of electrocoagulation process for the simultaneous removal of mercury, lead, and nickel from contaminated water, Environ. Sci. Pollut. Res., 19 (2012) 2734–2744.

[6] T. Wajima, Y. Umeta, S. Narita, K. Sugawara, Adsorption behavior of fluoride ions using a titanium hydroxide-derived adsorbent, Desalination, 249 (2009) 323–330.

[7] R. Kamaraj, P. Ganesan, S. Vasudevan, Removal of lead from aqueous solutions by electrocoagulation: isotherm, kinetics and thermodynamic studies, Int. J. Environ. Sci. Technol., 12 (2015) 683–692.

[8] I.A. Saleh, N. Zouari, M.A. Al-Ghouti, Removal of pesticides from water and wastewater: chemical, physical and biological treatment approaches, Environ. Technol. Innov., 19 (2020) 101026, doi: 10.1016/j.eti.2020.101026.

[9] G. Nacu, D. Şuteu, L. Tofan, C. Păduraru, L. Bulgariu, Removal of Zn(II) ions from aqueous solution by sorption using cellulose functionalized with reactive dyes as adsorbents, J. Environ. Manage., 18 (2019) 321–327.

[10] K. Chithra, D. Satheesh, K. Jayanthi, S. Vasanth Kumar, V. Muthulakshmi, K. Kalaivani, R. Saravanan, P. Sellam, Cobalt(II) Complexes of (E)-2-(2-Hydroxy-3-methoxybenzalidene)hydrazinecarbo(thio)amides: synthesis, FTIR studies and their antimicrobial activity, Chem. Data Collect. 32 (2021) 100652, doi: 10.1016/j.cdc.2021.100652.

[11] F.-X. Collard, J. Blin, A review on pyrolysis of biomass constituents: mechanisms and composition of the products obtained from the conversion of cellulose, hemicelluloses and lignin, Renewable Sustainable Energy Rev., 38 (2014) 594–608.

[12] M. Boonterm, S. Sunyadeth, S. Dedpakdee, P. Athichalinthorn, S. Patcharaphun, R. Mungkung, R. Techapiesancharoenkij, Characterization and comparison of cellulose fiber extraction from rice straw by chemical treatment and thermal steam explosion, J. Cleaner Prod., 134 (2016) 592–599.

[13] M. Carrier, A. Loppinet-Serani, C. Absalon, C. Aymonier, M. Mench, Degradation pathways of holocellulose, lignin and α-cellulose from *Pteris vittata* fronds in sub- and super critical conditions, Biomass Bioenergy, 43 (2012) 65–71.

[14] Y. Essaadaoui, M. Galai, M. Ouakki, L. Kadiri, A. Ouass, M. Cherkaoui, E. Housseine Rifi, A. Lebkiri, Study of the anticorrosive action of *Eucalyptus camaldulensis* extract in case of mild steel in 1.0 M HCl, 54 (2019) 431–442.

[15] J. Henschen, D. Li, M. Ek, Preparation of cellulose nanomaterials via cellulose oxalates, Carbohydr. Polym., 213 (2019) 208–216.

[16] M. Yao, Z. Wang, Y. Liu, G. Yang, J. Chen, Preparation of dialdehyde cellulose graftead graphene oxide composite and its adsorption behavior for heavy metals from aqueous solution, Carbohydr. Polym., 212 (2019) 345–351.

[17] R. Bouhdadi, M. El Moussaouiti, B. George, S. Molina, A. Merlin, Acylation of cellulose by 3-pyridinoyl chloride hydrochloride: application in the adsorption of lead Pb^{2+}, C.R. Chim., 14 (2011) 539–547.

[18] J. Bensalah, A. Habsaoui, A. Lebkiri, O. El Khattabi, E.H. Rifi, Investigation of the cationic resin Amberlite®IRC-50 as a potential adsorbent to remove the anionic dye methyl orange, Desal. Water Treat., 246 (2022) 280–290.

[19] L. Zheng, P. Meng, Preparation, characterization of corn stalk xanthates and its feasibility for Cd(II) removal from aqueous solution, J. Taiwan Inst. Chem. Eng., 58 (2016) 391–400.

[20] S. Cinti, V. Mazzaracchio, I. Cacciotti, D. Moscone, F. Arduini, Carbon black-modified electrodes screen-printed onto paper towel, waxed paper, and Parafilm M®, Sensors, 17 (2017) 2267, doi: 10.3390/s17102267.

[21] J. Gatabi, Y. Sarrafi, M.M. Lakouraj, M. Taghavi, Facile and efficient removal of Pb(II) from aqueous solution by chitosan-lead ion imprinted polymer network, Chemosphere, 240 (2020) 124772, doi: 10.1016/j.chemosphere.2019.124772.

[22] S. Bondock, A.A. El-Zahhar, M.M. Alghamdi, S.M.A.S. Keshk, Synthesis and evaluation of N-allylthiourea-modified chitosan for adsorptive removal of arsenazo III dye from aqueous solutions, Int. J. Biol. Macromol., 137 (2019) 107–118.

[23] Y. Essaadaoui, A. Lebkiri, E. Rifi, L. Kadiri, A. Ouass, Adsorption of lead by modified *Eucalyptus camaldulensis* barks: equilibrium, kinetic and thermodynamic studies, Desalination, 111 (2018) 267–277.

[24] J.-K. Kang, S.-C. Lee, S.-B. Kim, Enhancement of selective Cu(II) sorption through preparation of surface-imprinted mesoporous silica SBA-15 under high molar concentration ratios of chloride and copper ions, Microporous Mesoporous Mater., 272 (2018) 193–201.

[25] J. Yan, Y. Zhu, F. Qiu, H. Zhao, D. Yang, J. Wang, W. Wen, Kinetic, isotherm and thermodynamic studies for removal of methyl orange using a novel β-cyclodextrin functionalized graphene oxide-isophorone diisocyanate composites, Chem. Eng. Res. Des., 106 (2016) 168–177.

[26] Y. Essaadaoui, A. Lebkiri, E.H. Rifi, L. Kadiri, A. Ouass, Adsorption of cobalt from aqueous solutions onto Bark of Eucalyptus, Mediterr. J. Chem., 7 (2018) 145–155.

[27] J. Bensalah, M. Berradi, A. Habsaoui, M. Allaoui, H. Essebaai, O. El Khattabi, A. Lebkiri, E.-H. Rifi, Kinetic and thermodynamic study of the adsorption of cationic dyes by the cationic artificial resin Amberlite®IRC50, Mater. Today:. Proc., 45 (2021) 7468–7472.

[28] Y.G. Abou El-Reash, A.M. Abdelghany, K. Leopold, Solid-phase extraction of Cu^{2+} and Pb^{2+} from waters using new thermally treated chitosan/polyacrylamide thin films; adsorption kinetics and thermodynamics, Int. J. Environ. Anal. Chem., 97 (2017) 965–982.

[29] M. Allaoui, M. Berradi, J. Bensalah, H. Es-sahbany, O. Dagdag, S. Ibn Ahmed, Study of the adsorption of nickel ions on the sea shells of Mehdia: kinetic and thermodynamic study and mathematical modelling of experimental data, Mater. Today:. Proc., 45 (2021) 7494–7500.
[30] M.D. Meitei, M.N.V. Prasad, Adsorption of Cu(II), Mn(II) and Zn(II) by *Spirodela polyrhiza* (L.) Schleiden: equilibrium, kinetic and thermodynamic studies, Ecol. Eng., 71 (2014) 308–317.
[31] V.K. Gupta, A. Mittal, R. Jain, M. Mathur, S. Sikarwar, Adsorption of Safranin-T from wastewater using waste materials— activated carbon and activated rice husks, J. Colloid Interface Sci., 303 (2006) 80–86.
[32] M. Basu, A.K. Guha, L. Ray, Adsorption behavior of cadmium on husk of lentil, Process Saf. Environ. Prot., 106 (2017) 11–22.
[33] M. EL Alouani, S. Alehyen, M. EL Achouri, M. Taibi, Removal of cationic dye – methylene blue – from aqueous solution by adsorption on fly ash-based geopolymer, J. Mater. Environ. Sci., 9 (2018) 32–46.
[34] J. Bensalah, A. Habsaoui, B. Abbou, L. Kadiri, I. Lebkiri, A. Lebkiri, E. Housseine Rifi, Adsorption of the anionic dye methyl orange on used artificial zeolites: kinetic study and modeling of experimental data, Mediterr. J. Chem., 9 (2019) 311–316.
[35] S. Elbariji, M. Elamine, H. Eljazouli, H. Kabli, A. Lacherai, A. Albourine, Treatment and recovery of wood by-products. Application to the elimination of industrial dyes, C.R. Chim., 9 (2006) 1314–1321.
[36] J. Bensalah, A. El Amri, A. Ouass, O. Hammani, L. Kadiri, H. Ouaddari, S. El Mustapha, A. Zarrouk, A. lebkiri, B. Srhir, E.H. Rifi, Investigation of the cationic resin Am®IRC-50 as a potential adsorbent of Co(II): equilibrium isotherms and thermodynamic studies, Chem. Data Collect., 39 (2022) 100879, doi: 10.1016/j.cdc.2022.100879.
[37] Y. Wang, Y. Xie, Y. Zhang, S. Tang, C. Guo, J. Wu, R. Lau, Anionic and cationic dyes adsorption on porous poly-melamine-formaldehyde polymer, Chem. Eng. Res. Des., 114 (2016) 258–267.
[38] Z. Sun, Y. Liu, Y. Huang, G. Zeng, Y. Wang, X. Hu, L. Zhou, Effects of indole-3-acetic, kinetin and spermidine assisted with EDDS on metal accumulation and tolerance mechanisms in ramie (*Boehmeria nivea* (L.) Gaud.), Ecol. Eng., 71 (2014) 108–112.
[39] L. Mouni, D. Merabet, D. Robert, A. Bouzaza, Batch studies for the investigation of the sorption of the heavy metals Pb^{2+} and Zn^{2+} onto Amizour soil (Algeria), Geoderma, 154 (2009) 30–35.
[40] Q. Albert, L. Leleyter, M. Lemoine, N. Heutte, J.-P. Rioult, L. Sage, F. Baraud, D. Garon, Comparison of tolerance and biosorption of three trace metals (Cd, Cu, Pb) by the soil fungus *Absidia cylindrospora*, Chemosphere, 196 (2018) 386–392.
[41] R. Tabaraki, A. Nateghi, Multimetal biosorption modeling of Zn^{2+}, Cu^{2+} and Ni^{2+} by *Sargassum ilicifolium*, Ecol. Eng., 71 (2014) 197–205.
[42] J. Bensalah, M. Berradi, A. Habsaoui, O. Dagdag, A. El Amri, O. El Khattabi, A. Lebkiri, E.H. Rifi, Adsorption of the orange methyl dye and lead(II) by the cationic resin Amberlite®IRC-50: kinetic study and modeling of experimental data, J. Chem. Soc. Pak., 43 (2021) 535–545.
[43] S. Chen, J. Zhang, C. Zhang, Q. Yue, Y. Li, C. Li, Equilibrium and kinetic studies of methyl orange and methyl violet adsorption on activated carbon derived from *Phragmites australis*, Desalination, 252 (2010) 49–156.
[44] E. Haque, J.W. Jun, S.H. Jhung, Adsorptive removal of methyl orange and methylene blue from aqueous solution with a metal-organic framework material, iron terephthalate (MOF-235), J. Hazard. Mater., 185 (2011) 507–511.
[45] N.-E. Fayoud, S.A. Younssi, S. Tahiri, A. Abderrahman Albizane, Kinetic and thermodynamic study of the adsorption of methylene blue on wood ashes, J. Mater. Environ. Sci., 6 (2015) 3295–3306.
[46] S.M. Maliyekkal, K.P. Lisha, T. Pradeep, A novel cellulose–manganese oxide hybrid material by in situ soft chemical synthesis and its application for the removal of Pb(II) from water, J. Hazard. Mater., 181 (2010) 986–995.
[47] J.K. Bediako, W. Wei, Y.-S. Yun, Conversion of waste textile cellulose fibers into heavy metal adsorbents, J. Ind. Eng. Chem., 43 (2016) 61–68.
[48] V.A. Kozlov, T.E. Nikiforova, V.A. Loginova, O.I. Koifman, Mechanism of protodesorption—exchange of heavy metal cations for protons in a heterophase system of H_2O–H_2SO_4–MSO_4—cellulose sorbent, J. Hazard. Mater., 299 (2015) 725–732.
[49] N. Srivastava, A.K. Thakur, V.K. Shahi, Phosphorylated cellulose triacetate–silica composite adsorbent for recovery of heavy metal ion, Carbohydr. Polym., 136 (2016) 1315–1322.
[50] A. EL Amri, J. Bensalah, Y. Essaadaoui, I. Lebkiri, B. Abbou, A. Zarrouk, E.H. Rifi, A. Lebkiri, Elaboration, characterization and performance evaluation of a new environmentally friendly adsorbent material based on the reed filter (*Typha latifolia*): kinetic and thermodynamic studies and application in the adsorption of Cd(II) ion, Chem. Data Collect., 39 (2022) 100849, doi: 10.1016/j.cdc.2022.100849.
[51] J. Bensalah, A. Habsaoui, A. Lebkiri, O. El Khattabi, E.H. Rifi, Investigation of the cationic resin Amberlite®IRC-50 as a potential adsorbent to remove the anionic dye methyl orange, Desal. Water Treat., 246 (2022) 280–290.